

Original article Opposed-phase bone marrow imaging with low-field MRI -basic studies and initial clinical experience

Izumi TOGAMI, Seiichiro OHNO*, Nobuya SASAI,
Ayuko YUZURIO, Tetsuro SEI, Masatoshi TSUNODA,
Shiro AKAKI, Ikuo JOJA**, Yoshio HIRAKI

Dept. of Radiology, Faculty of Medicine

**Dept. of Medical Radiotechnology, Faculty of Health Science, Okayama University Medical School

*Central Division of Radiology, Okayama University Hospital

Abstract

We report our basic studies and discuss our initial clinical experience with opposed-phase imaging performed using a low-field MRI system for the examination of vertebral bone marrow lesions. MR imaging was performed using a 0.2-tesla resistive magnet. Signal reduction in opposed-phase images was observed when both fat and water were present in the same pixel. On the other hand, such signal reduction was not noted in in-phase or spin echo images. In all clinical cases, uninvolved bone marrow was depicted with low signal intensity in opposed-phase image. Contrast in opposed phase images was higher than that in corresponding spin echo images for both T1-weighted images (T1WI) and T2 or T2*-weighted images (T2/T2*WI) in many cases. The enhancement effect in opposed-phase images was almost the same as that in spin echo images.

Keywords: bone marrow, MRI, opposed phase, low magnetic field

Introduction

The usefulness of MRI for the evaluation of bone marrow lesion has been established. (1-23) MRI studies are performed for the detection of lesions, the depiction of surrounding structures, and the evaluation of therapeutic effect. The signal patterns and enhancement effects of the lesion are important factors in establishing the correct diagnosis. In low-field MRI studies, contrast of the lesion relative to uninvolved bone marrow and its enhancement effect are often poor. The chemical shift selective fat saturation (CHESS) method selectively suppresses fat signals (24-26) and is useful for depicting bone marrow lesions in T2-weighted images (T2WI) and postcontrast T1-weighted images (T1WI). (15,18,19) It is, however, impossible to use the CHESS method in low-field systems because the frequency difference between water and fat is small.

Opposed-phase images, in which the echo time is set so that water and fat are in opposite phases in a gradient echo sequence, can be employed in all clinical MRI systems. Such images are expected to be useful for the diagnosis of bone marrow lesions using low-field systems. There have been no reports on opposed-phase images in low-field MRI in the literature, although there have been several reports on the use of such images in high-field MRI. (2,6,10,13,22,23)

In the present study, we report our basic studies and describe our initial clinical experience with opposed-phase imaging performed using a low-field MRI system for the evaluation of vertebral bone marrow lesions.

Materials and methods

MR imaging was performed using a 0.2-tesla resistive magnet (Magnetom Open, Siemens, Erlangen, Germany) with a body-small coil.

Contact address of the principal author :

Izumi TOGAMI Dept. of Radiology, Okayama Univ. Medical School 2-5-1 Shikata-cho, Okayama-city, 700-8558
TEL. 086-235-7313 FAX.086-235-7316

Signal reduction in opposed-phase images was confirmed using a phantom in basic studies. Both fat and water were placed into the phantom, with baby oil used as the fat component. A small amount of Gd-DTPA was added to distilled water as the water component in order to ensure isointensity with fat in both T1WI and T2WI. (Afterwards, the T1 and T2 values of both components were measured. The T1 value of fat was 138 ms, and that of water was 95 ms, and the T2 value of fat was 80 ms and that of water was 73ms.) The ratio of fat to water was varied by changing the slice position. The slice thickness was 10mm, and five images were obtained: a)100% fat, b)75% fat and 25% water, c)50% fat and 50% water, d)25% fat with 75% water, and e)100% water. The signal intensity of the phantom and the standard deviation of the background were measured for each image, and the signal-to-noise ratio (SNR) was calculated for each phantom. The SNR was defined as the signal intensity value of the phantom divided by the standard deviation of the background. The basic studies included a spin echo sequence (T1 SE) and opposed-phase (T1 op.) and in-phase (T1 in) gradient echo sequences for T1WI and a turbo-spin echo sequence (T2 TSE) and opposed phase (T2* op.) and in-phase (T2* in) gradient echo sequence for T2/T2*WI. The sequence parameters are shown in **Table 1**.

In the clinical cases, the contrast of lesions relative to uninvolved bone marrow was evaluated in T1WI and T2/T2*WI, and the degree of enhancement in T1WI was assessed by the consensus of two radiologists. Eleven

patients (6 men, 5women) with vertebral lesions were included in this initial clinical study. The patients ranged from 4 to 72 years of age (average age, 53.3years). The diagnosis was bone metastasis in 7 patients, post-radiotherapy for bone metastasis in 2, vertebral hemangioma in 1, and osteoarthritis in 1. The diagnosis was based on clinical findings, the patients clinical course, and the results of other imaging examinations. No histological corroboration was obtained. T1 SE and T2 TSE were performed as precontrast studies and T1 SE was performed after the administration of contrast medium. One or two of the three opposed-phase images (T1 op., T2* op., and

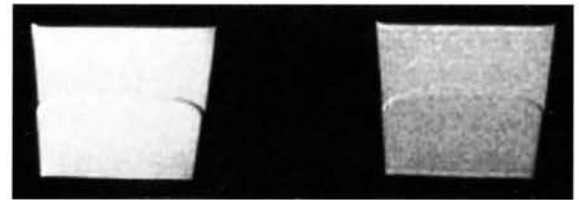


Figure 1. Coronal images of the phantom
left: T1 SE, right: T2 TSE

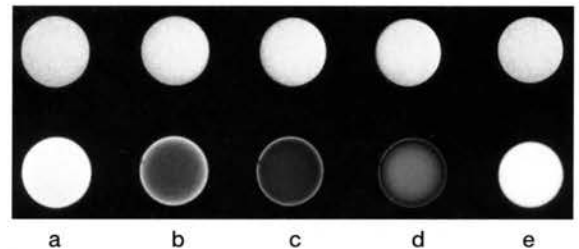


Figure 2. Axial images of the phantom
a: 100% fat b: 75% fat and 25% water
c: 50% fat and 50% water d: 25% fat and 75% water
e: 100% water

Each T1 SE image shows similar signal intensity, but T1 op. images including both fat and water in the same slice (lower: b,c,d) show low signal intensity.

Table1. Sequence parameters

| Sequence | TR (msec.) | TE (msec.) | Flip angle (deg.) | ETL | Acquisition | Bandwidth (Hz/pixel.) | Scanning time |
|----------|---------------|---------------|----------------------|-----|-------------|--------------------------|---------------|
| T1 SE | 500 | 30 | | | 2 | 33 | 5min.10sec. |
| T2 TSE | 6000 | 114 | | 7 | 1 | 65 | 9min.19sec. |
| T1 op. | 500 | 17 | 90 | | 2 | 56 | 5min.10sec. |
| T2*op. | 500 | 17 | 25 | | 2 | 56 | 5min.10sec. |
| T1 in | 500 | 35 | 90 | | 2 | 26 | 5min.10sec. |
| T2*in | 500 | 35 | 25 | | 2 | 26 | 5min.10sec. |

Slice thickness=10mm, Matrix=192×256, Field of view=320mm
ETL:echo train length

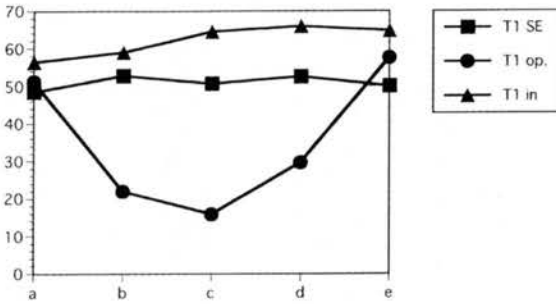


Figure 3a

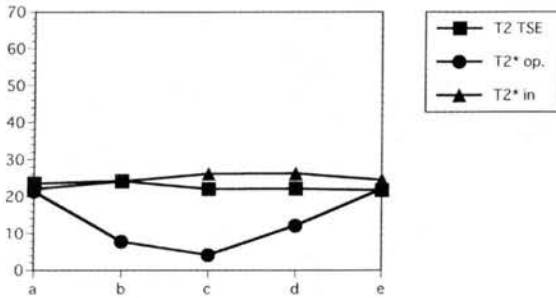


Figure 3b

Figure 3. Signal-to-noise ratio (SNR) of each image
a: T1WI, b: T2/T2*WI

The SNR is reduced in opposed-phase images when both fat and water are present in the same pixel. The SNR of in-phase images, which is similar to that of spin echo images, is not reduced even when both fat and water are present in the same pixel. The image of 50% fat and 50% water shows the lowest signal intensity of all the images. The SNR of T1WI is about three times higher than that of corresponding T2/ T2*WI.

postcontrast T1 op.) were also obtained within a reasonable examination time.

Results

In coronal phantom images (figure 1), the signal intensities of fat and water were similar in both T1 SE and T2 TSE. Figure 2 shows five images obtained by T1 SE and T1 op. Each T1 SE image shows similar signal intensity, but some T1 op. images including both fat and water in the same slice (lower: b,c,d) show low signal intensity. Figure 3 shows the SNR of T1WI, and T2/T2*WI. The SNR is reduced in opposed-phase images when both fat and water are contained in the same slice. The SNR of in-phase images is not reduced and is similar to that of spin echo

images.

In all of the clinical cases, uninvolved bone marrow showed low intensity in opposed-phase image. Table 2 shows the results of visual evaluation in each examination. In many cases, the contrast in opposed-phase images was higher than that in the corresponding spin echo images for both T1WI and T2/T2*WI, although it should be noted only a small number of clinical cases were evaluated in this study. The degree of enhancement in opposed-phase images was almost the same as that in spin echo images.

Several illustrative clinical cases are presented. Case 1 is a 33-year-old man with bone metastases from testicular cancer (figure 4a-e). A metastatic lesion in the spinous process of the ninth thoracic vertebra is more clearly demonstrated in a T1 op. image than in T1 SE and T2 TSE images, and enhancement is more pronounced. Case 2 is a 70-year-old woman who underwent radiotherapy for bone metastasis from breast cancer (figure 5a-c). Post-radiation fatty changes from the second to the fourth lumbar vertebra and another metastatic lesion in the eleventh thoracic vertebra are more clearly depicted in a T1 op. image than in T1 SE or T2 TSE images. The next example is a case in which the contrast of the lesion was not improved in opposed-phase imaging compared with the SE method. Case 3 is a 71-year-old man with sclerotic bone metastases

| | A | B | C |
|-------------------|---|---|---|
| T1WI | 4 | 3 | 0 |
| T2/T2*WI | 3 | 1 | 1 |
| postcontrast T1WI | 1 | 3 | 1 |

Table 2. Visual evaluation of each imaging technique For T1WI and T2/T2*WI, contrast of the lesion relative to uninvolved bone marrow was evaluated. For postcontrast T1WI, the degree of enhancement was assessed.

A: Clearer in opposed-phase images

B: Equally clear

C: Clearer in spin echo images

Contrast in opposed phase images is higher than that in corresponding spin echo images for both T1WI and T2/T2*WI. The degree of enhancement in opposed-phase images is almost the same as that in spin echo images.

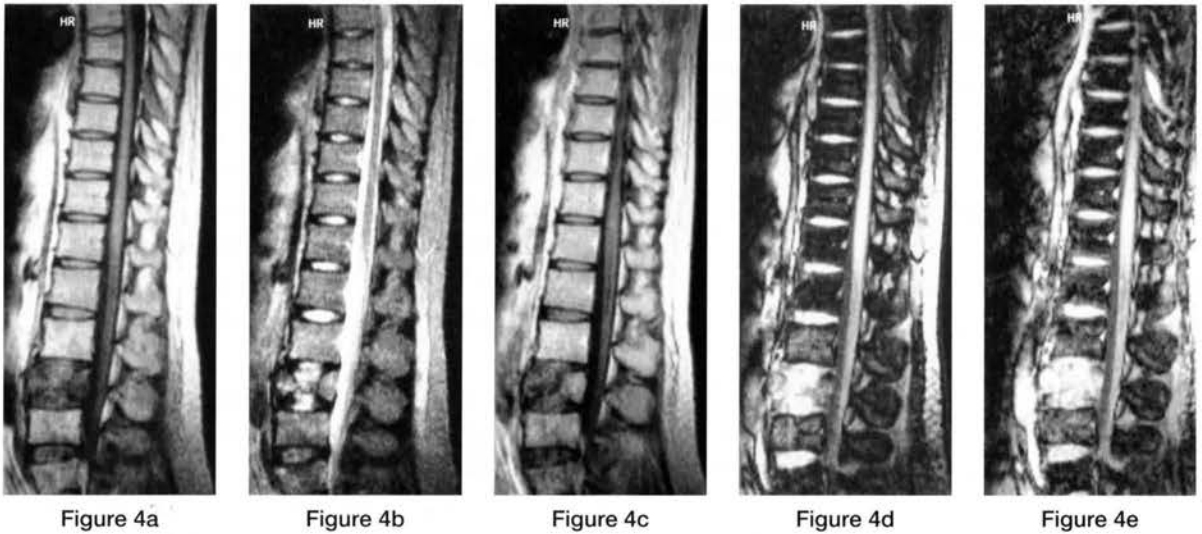


Figure 4 33-year-old man with bone metastases from testicular cancer

a: T1 SE, b: T2 TSE, c: postcontrast T1 SE, d: T1 op., e: postcontrast T1 op.

Compression fracture of the fourth lumbar vertebra is recognized. The lesion shows low signal intensity in a T1 SE image (a), isointensity in a T2 TSE image (b), and slight enhancement in the posterior part of the vertebral body (c). Another metastatic lesion in the spinous process of the ninth thoracic vertebra is clearly demonstrated in a T1 op. image (d), and enhancement is also clearly observed (e), whereas the lesion is not clearly visualized in T1 SE and T2 TSE images.

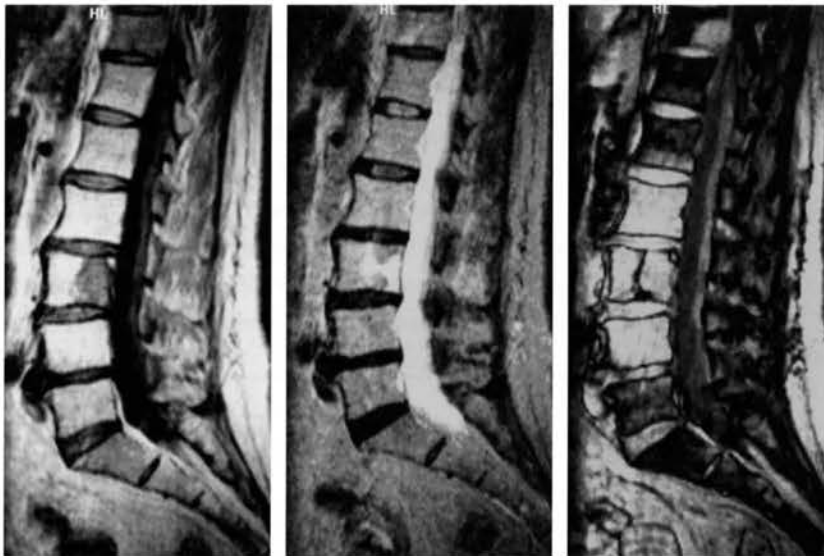


Figure 5

70-year-old woman who underwent radiotherapy for bone metastasis from breast cancer

a: T1 SE, b: T2 TSE, c: T1 op.

A metastatic lesion in the third lumbar vertebra is clearly depicted in both T1 SE (a) and T2 TSE (b) images, whereas fatty marrow showing post-radiation changes from the second to the fourth lumbar vertebra and another metastatic lesion in the eleventh thoracic vertebra are clearly shown in a T1 op. image (c).

from prostatic cancer (figure 6a-c). Bone metastatic lesions are depicted as low signal intensity in all images. In T2* op. images, contrast between the lesion and uninvolved bone marrow is reduced. Case 4 is a 61-year-old man with prostatic cancer. Since he complained of

backache, MRI was performed for suspected bone metastasis (figure 7a-c). As small lesion in the first lumbar vertebral body shows high signal intensity in both T1 SE and T2 TSE images, and is therefore identified as a hemangioma. In a T1 op. image, the lesion is also depicted as an area of



Figure 6a



Figure 6b



Figure 6c

Figure 6 71-year-old man with sclerotic bone metastases from prostatic cancer

a: T1 SE, b: T2 TSE, c: T2* op. Extensive sclerotic metastatic bone lesions are depicted as low signal intensity in all images (a-c). In a T2* op. image, the signal of uninvolved bone marrow also shows low signal intensity, so contrast between the lesion and uninvolved bone marrow is reduced (c).



Figure 7a



Figure 7b



Figure 7c

Figure 7 61-year-old man with prostatic cancer

a: T1 SE, b: T2 TSE, c: T1 op.

This patient complained of backache, and MRI was performed for suspected bone metastasis (a-c). A small lesion is seen in the first lumbar vertebral body. Since the lesion shows high signal intensity in both T1 SE (a) and T2 TSE (b) images, it is identified as a hemangioma. In a T1 op. image (c), the lesion also shows high signal intensity. It is considered difficult to differentiate between metastases and other lesions based on opposed-phase images alone.

high signal intensity. It is considered difficult to differentiate between metastases and other lesions based on opposed-phase images alone.

Discussion

Bone scintigraphy is widely employed for the detection of bone metastases. However, non-metastatic lesions such as fractures or areas of inflammation sometimes show high uptake. MRI is an excellent diagnostic modality for examining

soft tissues and is useful for the evaluation of lesions showing high uptake in bone scintigraphy.^(20,21) Differentiation between a fracture secondary to osteoporosis and a fracture secondary to metastasis is particularly important when compression fracture of a vertebral body is found.^(16,17) The morphological characteristics, signal pattern, and enhancement effect of the lesion are important factors in establishing the correct diagnosis. MRI is also useful for evaluating the relationship between tumors and nearby structures such as the spinal cord and nerve roots. In addition, MRI makes it possible to estimate the area of involvement in diseases that spread within the bone marrow such as leukemia and multiple myeloma.^(4,7,10,11,13,14) The usefulness of MRI in the evaluation of bone marrow lesions has been widely recognized.⁽¹⁻²³⁾

However, in examinations performed using low-field MRI systems, lesions often show low contrast and poor enhancement relative to uninvolved areas. In T1WI, the echo time (TE) must be set longer in order to set a longer sampling time to compensate for the low SNR, and T1 contrast is degraded as a result. In T2 TSE, which is currently widely employed for routine scanning, uninvolved bone marrow is depicted as high signal intensity compared with conventional T2-weighted spin echo sequences. Therefore, contrast between uninvolved bone marrow and lesions, which are usually depicted as areas of high signal intensity, is degraded. With respect to enhancement effects, there are two disadvantages in low-field MRI. One is poor T1 contrast due to the relatively long TE. The other is that the T1 value in low-field MRI studies is shorter than that in high-field studies, which means that after the administration of contrast medium, the degree of shortening in the T1 value is reduced. The usefulness of fat suppression method, in addition to routine T1- and T2-weighted imaging, has been established for bone marrow lesions. Although there are several fat suppression methods available, the CHESSE method⁽²⁴⁻²⁶⁾ is widely employed for the

examination of the bone marrow in mid- or high-field MRI studies.^(15,18,19) In this method, signals are obtained after fat is selectively saturated, and a high field is advantageous due to large frequency difference between water and fat. However, the frequency difference is only about 28 Hz at 0.2 tesla, so it is impossible to employ the CHESSE method in a 0.2-tesla MRI system. The short TI inversion recovery (STIR) method is another fat suppression method that is available in all clinical systems. The disadvantages of this method are a low SNR and different contrast effects from the SE method. Enhancement is also difficult to evaluate in this method.

Opposed-phase imaging is also available in all clinical MRI systems. The difference in resonance frequency between water and fat is about 3.5ppm. In gradient echo sequences, various directions of water and fat can be specified in relation to the echo time. Among these directions, in-phase is defined as the case when water and fat are in the same direction, and opposed phase is defined as the case when water and fat are in opposite directions. When only one component is present in a pixel, the intensity represents the signal of the component itself. However, when both fat and water are present in the same pixel, the signal intensity represents the sum of the two components in in-phase images and the difference in opposed-phase images. Therefore, in opposed-phase images, tissues that contain both water and fat show low signal intensity and tissues that contain only water or fat show high signal intensity, as demonstrated in our basic studies. This is a major difference from the CHESSE and STIR methods. Cycling between in-phase and opposed-phase condition is slow in a 0.2-tesla system, with the first opposed-phase condition appearing at about 17.5 ms and the first in-phase condition appearing at about 35 ms. In our clinical studies, TE was set to 17 ms for opposed-phase images.

In the basic studies described here, the ratios of the components in the phantom were varied using the partial volume effect by changing the

slice position, and the resulting changes in signal intensity were evaluated. Signal reduction was observed when both fat and water were present in opposed-phase images. Both fat and water components were liquid, and the boundary surface was not straight due to surface tension effects. As a result, concentric circles were seen in the images, and ratios did not agree perfectly with theoretical values. Nevertheless, changes in signal intensity could be clearly observed.

Bone marrow can be divided into red bone marrow and fatty yellow marrow, with the amount of yellow marrow gradually increasing with age. The composition of red marrow is 40% water, 40% fat, and 20% protein, while yellow marrow contains 15% water, 80% fat, and 5% protein.⁽⁵⁾ It is therefore expected that the signal from red marrow should be strongly suppressed in opposed-phase images. In adults, red marrow tends to persist in the vertebral bodies, while the red marrow in distal parts of the long bones is converted to yellow marrow.^(1,9) Therefore, vertebral bone marrow shows low signal intensity in opposed-phase images in both children and adults. Although a large number of subjects of various ages should be studied before reaching a firm conclusion, the bone marrow showed low signal intensity in opposed-phase images in all of the cases in the present study. Bone metastases usually arise in red marrow due to hematogenous spread, and the detection of metastases in the spine is of great clinical importance.

Although the present study included only a small number of cases, lesions containing a large water component such as metastases were depicted as high signal intensity, and contrast relative to uninvolved areas was good. However, since sclerotic metastatic lesions show low signal intensity in opposed-phase images, contrast is reduced, as shown in case 3. In this case, routine T1 SE and T2 TSE images were useful, and it was not necessary to obtain opposed-phase images. Lesion containing large amounts of fat show high signal intensity in opposed-phase images, as shown in case 4.^(3,8,12) In such cases as

well, opposed-phase images do not need to be obtained, since routine T1WI and T2WI are adequate for diagnosis. Therefore, opposed-phase imaging should not replace routine T1 SE and T2 TSE, but should be used in combination in order to improve the detectability of the lesions.

The advantages and disadvantages of opposed-phase images can be summarized as follows. The advantages are 1) such images can be obtained even using a low-field MRI system, 2) both T1- and T2-weighted images can be obtained, 3) contrast is good, resulting in high sensitivity in the detection of lesions, and 4) enhancement effects can be evaluated. The disadvantages are 1) the SNR of opposed-phase images is low and 2) other types of images must be acquired to ensure a correct diagnosis, since areas of high signal intensity may appear for a variety of reasons. In conclusion, our initial experience indicates that opposed-phase images show great promise in the diagnosis of bone marrow lesions with low-field MRI.

References

1. Dooms GC, Fisher MR, Hricak H, et al: Bone Marrow Imaging: Magnetic Resonance Studies Related to Age and Sex. *Radiology* 155; 1985: 429-432.
2. Wismer GL, Rosen BR, Buxton R, et al: Chemical shift imaging of bone marrow: Preliminary experience. *AJR* 145; 1985: 1031-1037.
3. Hajek PC, Baker LL, Goobar JE, et al: Focal Fat Deposition in Axial Bone Marrow: MR Characteristics. *Radiology* 162; 1987: 245-249.
4. McKinstry CS, Steiner RE, Young AT, et al: Bone marrow in leukemia and aplastic anemia: MR imaging before, during and after treatment. *Radiology* 162; 1987: 701-707.
5. Vogler JB, Murphy WA: Bone Marrow Imaging. *Radiology* 168; 1988: 679-693.
6. Rosen BR, Fleming DM, Kushner DC, et al: Hematologic Bone Marrow Disorders: Quantitative Chemical Shift MR Imaging. *Radiology* 169; 1988: 799-804.

7. Dohner H, Guckel F, Knauf W, et al: Magnetic resonance imaging of bone marrow in lymphoproliferative disorders: Correlation with bone marrow biopsy. *Br J Haematol* 73; 1989 : 12 -17.
8. Stevens SK, Moore SG, Kaplan ID: Early and late bone marrow changes after irradiation: MR evaluation. *AJR* 154 ; 1990 : 745-750.
9. Ricci C, Cova M, Kang YS, et al: Normal Age-related Patterns of Cellular and Fatty Bone Marrow Distribution in the Axial Skeleton: MR Imaging Study. *Radiology* 177; 1990 : 83-88.
10. Guckel F, Brix G, Semmier W, et al: Systemic bone marrow disorders: Characterization with proton chemical shift imaging. *J Comput Assist Tomogr* 14 ; 1990 : 633-642.
- Hoane BR, Shields AF, Porter BA, et al:
11. Detection of lymphomatous bone marrow involvement with magnetic resonance imaging. *Blood* 78 ; 1991 : 728-738.
12. Yankelevitz DF, Henschke CI, Knapp PH, et al : Effect of radiation therapy on thoracic and lumbar bone marrow : Evaluation with MR imaging. *AJR* 157; 1991 : 87-92.
13. Gerard EL, Ferry JA, Mmrein P, et al: Compositional changes in vertebral bone marrow during treatment for acute leukemia: Assessment with quantitative clinical shift imaging. *Radiology* 183 ; 1992 : 39 - 46.
14. Steiner RM, Mitchell DG, Rao VM, et al: Magnetic Resonance Imaging of Diffuse Bone Marrow Disease. *Radiol Clin North Am* 31 ; 1993 : 383-409.
15. Mirowitz SA, Apicella P, Reinus WR, et al: MR imaging of bone marrow lesions: relative conspicuousness on T1-weighted, fat-suppressed T2-weighted, and STIR images. *AJR* 162 ; 1994 : 215-221.
16. Fujii M, Kono M: Diagnostic imaging of the spine with emphasis on MRI. *Japanese Journal of Tomography* 21; 1995 : 133-141. (In Japanese)
17. Cùod CA, Laredo JD, Chevret S, et al: Acute Vertebral Collapse Due to Osteoporosis or Malignancy: Appearance on Unenhanced and Gadolinium-enhanced MR Images. *Radiology* 199; 1996: 541-549.
18. Chrysikopoulos H, Pappas J, Papanikolaou N, et al : Bone marrow lesions : evaluation with fat-suppression turbo spin echo MR imaging at 0.5T. *Eur. Radiol.* 6 ; 1996 : 895 - 899.
19. Georgy BA, Hesselink MJR, Middleton MS: Quantitative analysis of signal intensities and contrast after fat suppression in contrast-enhanced magnetic resonance imaging of the supine. *Acad. Radiol* 3 ; 1996 : 731 - 734.
20. Yuleung C, Kamwing C, Waiman L, et al: Comparison of whole body MRI and radioisotope bone scintigram for skeletal metastases detection. *Chinese Medical Journal* 110; 1997 : 485 - 489.
21. Eustace S, Tello R, DeCarvalho V, et al: A Comparison of Whole-Body TurboSTIR MR Imaging and Planar ^{99m}Tc-Methylene Diphosphonate Scintigraphy in the Examination of Patients with Suspected Skeletal Metastases. *AJR* 169 ; 1997 : 1655-1661.
22. Disler DG, McCauley TR, Ratner LM, et al: In-Phase and Out-of-Phase MR Imaging of Bone Marrow: Prediction of Neoplasia Based on the Detection of Coexistent Fat and Water. *AJR* 169 ; 1997 : 1439-1447.
23. Seiderer M, Staebler A, Wagner H: MRI of bone marrow: opposed-phase gradient-echo sequences with long repetition time. *Eur. Radiol* 9 ; 1999 : 652-661.
24. Haase A, Frahm J, Hanicke W, et al: 1H NMR chemical shift selective (CHESS) imaging. *Phys Med Biol* 30 ; 1985 : 341-344.
25. Keller PJ, Hunter WW, Schmalbrok P: Multisection fat-water imaging with selective presaturation *Radiology* 164 ; 1987 : 539-541.
26. Chan TW, Listerud J, Kressel HY, et al: Combined Chemical-Shift and Phase-Selective Imaging for Fat Suppression: Theory and Initial Clinical Experience. *Radiology* 181; 1991 : 41-47.

ダウンロードされた論文は私的利用のみが許諾されています。公衆への再配布については下記をご覧ください。

複写をご希望の方へ

断層映像研究会は、本誌掲載著作物の複写に関する権利を一般社団法人学術著作権協会に委託しております。

本誌に掲載された著作物の複写をご希望の方は、(社)学術著作権協会より許諾を受けて下さい。但し、企業等法人による社内利用目的の複写については、当該企業等法人が社団法人日本複写権センター（(社)学術著作権協会が社内利用目的複写に関する権利を再委託している団体）と包括複写許諾契約を締結している場合にあっては、その必要はございません（社外頒布目的の複写については、許諾が必要です）。

権利委託先 一般社団法人学術著作権協会

〒107-0052 東京都港区赤坂 9-6-41 乃木坂ビル 3F FAX：03-3475-5619 E-mail：info@jaacc.jp

複写以外の許諾（著作物の引用、転載、翻訳等）に関しては、(社)学術著作権協会に委託致しておりません。

直接、断層映像研究会へお問い合わせください

Reprographic Reproduction outside Japan

One of the following procedures is required to copy this work.

1. If you apply for license for copying in a country or region in which JAACC has concluded a bilateral agreement with an RRO (Reproduction Rights Organisation), please apply for the license to the RRO.

Please visit the following URL for the countries and regions in which JAACC has concluded bilateral agreements.

<http://www.jaacc.org/>

2. If you apply for license for copying in a country or region in which JAACC has no bilateral agreement, please apply for the license to JAACC.

For the license for citation, reprint, and/or translation, etc., please contact the right holder directly.

JAACC (Japan Academic Association for Copyright Clearance) is an official member RRO of the IFRRO (International Federation of Reproduction Rights Organisations).

Japan Academic Association for Copyright Clearance (JAACC)

Address 9-6-41 Akasaka, Minato-ku, Tokyo 107-0052 Japan

E-mail info@jaacc.jp Fax: +81-33475-5619